DENDROBIOLOGY

2024, vol. 91, 85–99

https://doi.org/10.12657/denbio.091.007

*Hongying Tang, Fan Miao, Jie Yang, Bingyu Wu, Qi Zhang, Hongke Hao**

Considering the composite tree attributes extracted by UAV can improve the accuracy of street tree species classification

Received: 8 January 2024; Accepted: 27 March 2024

Abstract: Identifying simple tree attributes of street trees, i.e., tree height, crown width and crown height obtained by unmanned aerial vehicles (UAV), plays a significant role in urban management to maximize the ecological benefits of street trees. However, simple attributes usually fluctuate over a wide range due to differences in tree-age and growing environment, leading to inconspicuous interspecific features and low classification accuracy. Composite attributes, expressed by two or more simple attributes, can be used to reduce the variability in simple tree attributes, thus providing an alternative to improve the accuracy of street tree classification. In this study, we examined the classification effects of simple attributes and simple-composite attribute combinations by back propagation (BP) neural network, K-nearest neighbor (KNN) and support vector machine (SVM). The results showed that (1) the values obtained by UAVs and observations were highly consistent and R^2 values for tree height, east-west crown width, north-south crown width and crown height were 0.90, 0.87, 0.78 and 0.76, respectively. The relative errors of tree height were the most stable among different tree species, followed by the crown height, east-west crown width and north-south crown width. (2) Compared to simple attributes, composite attributes displayed significant differences among street tree species, and these differences were helpful for identifying street tree species that could not be identified with simple attributes. (3) The accuracy of tree species identification after including corresponding composite attributes can be improved by 29.7% (kappa coefficient improved by 0.34) compared with only using simple attributes. The results suggested that consideration of composite attributes in street tree species classification reduced the mistakes for identifying tree species, thus providing a new approach for identifying street tree species and managing street trees efficiently.

Keywords: tree species classification; street trees; composite attributes; machine learning algorithm; UAV

Addresses: H. Tang, F. Miao, J. Yang, B. Wu, Hao H, College of Forestry, Northwest A&F University, Yangling 712100, China, e-mail: hhk2018@126.com
Q. Zhang, College of information engineering, Northwest A&F University, Yangling 712100, China
* corresponding author

Introduction

Street trees, as important parts of urban ecosystems, play valuable roles in reducing air temperature, improving the environment, and reducing city noise (Aval et al., 2018). For example, when street tree cover increases by 1% over an area of 300 × 300 m^2, the mean radiant temperature will decrease by 3.2–6.3 °C in the daytime (Aminipouri et al., 2019a; Aminipouri et al., 2019b). However, for urban forest management, the ecological functions of different species are often ignored leading to potential pest and disease outbreaks for specific trees (Zong et al., 2020). For instance, street trees such as *Acer* spp. are favourites of the Asian longhorned beetle, and if the population of *Acer* spp. gets too large, extensive street trees will die or have to be removed (Cowett & Bassuk, 2020). Additionally, some evidence has shown that identifying street trees can improve the efficiency of preventing pollen allergies. An increase in species richness of street trees can lead to pollen allergens, which were found to be significantly correlated with increased asthma hospitalization (Lai & Kontokosta, 2019). Therefore, the identification of street trees plays an important and indispensable role in urban forest management to improve the resistance of street trees and reduce the pollen allergy risk of residents (Aval et al., 2018).

Unmanned aerial vehicles (UAVs), positioned at the forefront of remote sensing technologies, are extensively utilized in forest monitoring and classification to directly capture basic attributes (such as tree height, crown width, crown height, and tree diameter) of street trees, facilitating the rapid acquisition of information within a concise timeframe (Charron et al., 2020; Schiefer et al., 2020). Of these attributes, tree height stands out as the most readily extractable, with errors as minimal as 10% and a high coefficient of determination (R^2) reaching 0.80 (Hao et al., 2021; Jin et al., 2020).The most common application of UAVs is to assess tree growth by assessing measuring tree height (Qin et al., 2022). Similarly, the crown diameter can be measured with an error of less than 10% and R^2 values as much as 0.90, which, in turn, can be used to derive tree stand accumulation metrics and evaluate ecological benefits at large scales (Dong et al., 2020; Nasiri et al., 2021). One of the limitations of traditional measurement is that the accuracy of street trees is highly dependent on the professional experience of surveyors and manual surveys are often time-consuming and laborious (Da-tong, 2015). Conversely, measuring the simple attributes of street trees with UAVs is helpful for accurate street tree information collection in a short time and hence improving urban forest management efficiency (Zhou et al., 2022).

Simple attributes are often used to identify trees of the same age grown in a similar environment, but some limitations exist in identifying street trees of different ages and grown under different environments. For example, simple attributes of a tree species can highly vary for trees at different ages, thus increasing intraspecific differences and decreasing interspecific differences. These issues can lead to confusion between relevant attributes and the attributes of other tree species, resulting in low classification accuracy (R^2 commonly lower than 0.7) (Guo et al., 2022; Choudhury et al., 2020; Sawaid et al., 2021). In addition to tree age, the locations of trees, tree pit size, adjacent land use, the presence or absence of tree grates or guards and the width of sidewalks can result in fluctuations in measurements of simple attributes of the same tree species (Ow et al., 2018; Tan & Shibata, 2022). Due to these intraspecific differences, simple attributes may not be effective for identifying street tree species, and more types of attributes are suggested in the classification process.

Composite attributes were developed based on two or more simple attributes in a proportional approach to reduce the possibility of confusion among trees (Kraidech & Jearanaitanakij, 2017). The accuracy of street tree identification depends on intraspecific similarity and interspecific differences. For a tree species, due to differences in age and environment, simple attributes vary but the corresponding tree shapes (expressed based on the proportion of simple attributes) are similar and thus can be used as stable indicators in classification (Chen et al., 2009). Composite attributes can be effectively clustered, thus reducing the confusion among species and improving the accuracy of tree species identification (Duizer et al., 1997).

The choice of classifiers has a significant effect on street tree identification (Michałowska & Rapiński, 2021). The K-nearest neighbor (KNN), support vector machine (SVM) and back propagation (BP) neural network methods are widely used to identify street tree species and the accuracy can achieve of approximately 70% (Franklin & Ahmed, 2018; Raczko & Zagajewski, 2017; Zhang et al., 2021). The KNN classifier is suitable for analyzing large-size samples but can produce poor results when classifying small-size samples, with an accuracy of less than 70% (Zhang et al., 2006). SVMs perform well in cases with low-quality samples, but overfitting can occur when the sample size is small, resulting in a maximum accuracy of approximately 60% (Jombo et al., 2021; Pu & Landry, 2012). BP neural networks provide strong nonlinear mapping ability and a flexible network structure, yielding a satisfactory classification effect for both small and large samples, but overfitting occurs sometimes (Fassnacht et al., 2016). Nonetheless, machine learning methods,

which perform well for random samples, can reduce uncertainty in classification tasks.

In this study, we compared the differences in tree attributes between using composite attributes and simple attributes. High-accuracy tree species identification algorithms were applied to efficiently identify street trees. Four simple attributes, namely, tree height (H), the length of the crown in the east-west direction (L_x), the length of the crown in the north-south direction (L_y) and crown height (H_c), were combined to form eight composite attributes (L_x/H, L_y/H, H_c/H, L_x/H_c, L_y/H_c, L_x/ L_y, crown surface area(S), and crown volume (V)), and the differences in attributes were compared for different tree species. Simple attributes and simple-composite attribute combinations were used in identifying street trees by BP neural network, KNN and SVM. The objectives of this study were to (1) explore the accuracy of the tree attributes extracted by UAVs; (2) verify that tree species exhibit more differences based on composite attributes than that of simple attributes; and (3) compare the accuracy of tree species identification based on simple attributes andsimple-composite attribute combinations .

Materials and methods

Study area

Yangling (34°16'56.24"N, 108°4'27.95"E) is located in the western part of the central Guanzhong Plain in Shaanxi Province China at an altitude of 435–563 meters. The amount of annual precipitation and average annual temperatures are 635.1–663.9 mm and 12.9°C, respectively. Precipitation is mostly concentrated in July and September (Fig. 1a). The UAV data in the study area was collected by the Dajiang Spirit 4RTK (Fig. 1b). Various street trees in the study area, such as *Koelreuteria paniculata*, *Aesculus chinensis*, *Catalpa bungei*, *Liriodendron chinense*, *Ginkgo biloba* and *Firmiana platanifolia*, are the most common northern tree species (Li, 2022; Zhang, 2020) (Fig. 1c).

Technical roadmap

To meet the research objectives, three steps were designed (Fig. 2). First, the effectiveness of tree attribute extraction based on UAVs is tested through correlation analyses between the extracted and observed simple attributes obtained by Total Station. The model of total station used in this research is

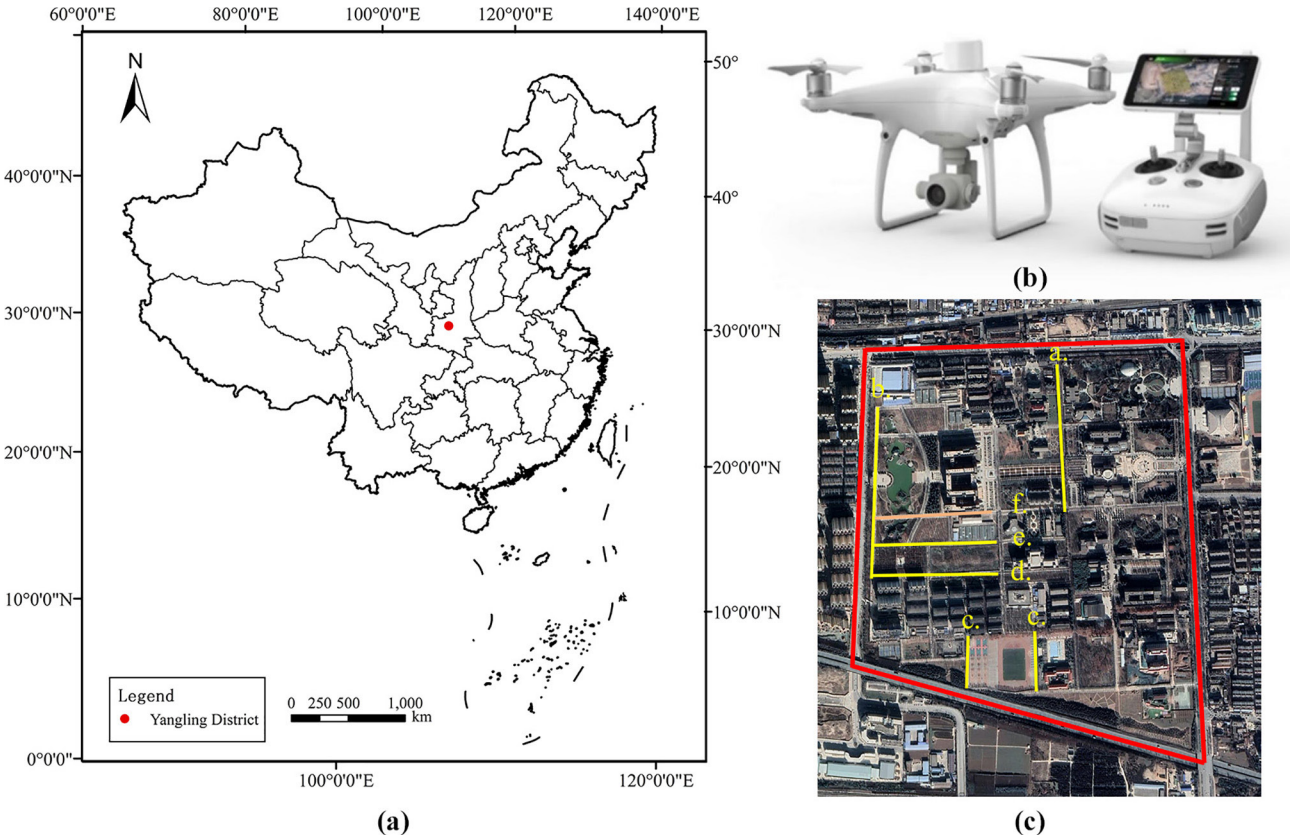

Fig. 1. Location of the study area. Panel (a) is the location of the study area in China; Panel (b) is the Dajiang Spirit 4RTK (Image source: http://www.efuav.com/productinfo/19173.html?templateId=1133605), and different numbers in yellow in Panel (c) are the roads along which the six studied street tree species are located. *Koelreuteria paniculata*, *Aesculus chinensis*, *Catalpa bungei*, *Liriodendron chinense*, *Ginkgo biloba* and *Firmiana platanifolia* are labelled as a–f, respectively

South NTS −372R10 (mm+1×10^{-6}·D). Three-dimensional information was obtained from the spatial information in photos and Camera parameters by air-encrypted processing to obtain point cloud data by Context Capture 10.18 software. Simple attributes were extracted by LiDAR360 V5.4.2.0 software.The observations of simple attributes (H, L_x, L_y and H_c) were obtained with Total Station, and the observations of S and V were obtained with the geometric method (Dai, 2015). Second, the effectiveness of the characterization of street trees based on simple and composite attributes was compared with Kruskal-Wallis test. Third, the classification accuracy was juxtaposed between basic attributes alone and

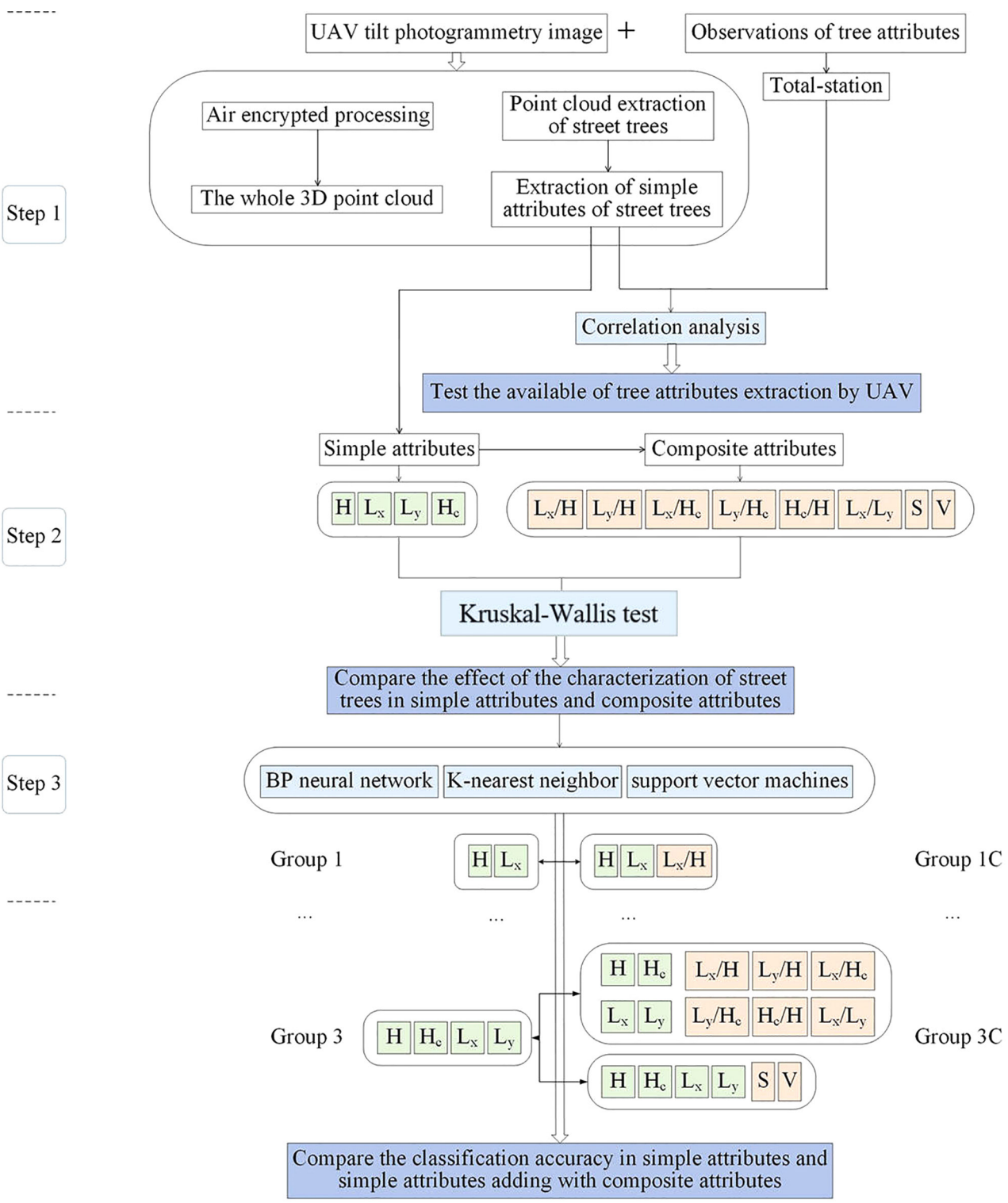

Fig. 2. Technical roadmap of this study

their amalgamation with pertinent composite attributes, employing BP neural network, KNN, and SVM to evaluate the classification precision of the suggested model.

Parameter setting and data processing

Firstly, the six attributes of street trees were obtained through a combination of manual acquisition and software extraction. Simple attributes for 90 street trees were collected by a UAV with a route plan based on five-way flight and a flight altitude of 50 m with a maximum flying speed of 7 m/s and heading overlap rate being 80% and a side overlap rate of 80%. Tilting photography, POS data and camera parameters were used for aerial triangulation High-density digital point clouds were obtained through the dense matching of multiview images (Navarro et al., 2020; Nevalainen et al., 2017; Su & Gao, 2020). Finally, the point cloud data of the whole study area is generated. A point cloud editor (LiDAR360 V5.4.2.0) was used to manually process the point cloud data. The data for six kinds of street trees (15 of each species, a total of 90 trees) were retained while others were ignored. The simple attribute data were obtained from the single-tree point clouds. H, S and V can be extracted by an automatic faction of LiDAR360. The point cloud data was imported into LiDAR360 with three-dimensional coordinates. The directions of the x and y axes in the three-dimensional coordinates correspond to the east-west and north-south directions in the geographic coordinates. When extracting the crown width, the point cloud was projected onto a two-dimensional x-y plane for measurement. The crown height is projected onto the x-z plane or the y-z plane for measurement (Table 1). The geometric method was used to approximate the tree crown based on regular geometry and calculate the surface area and volume of each tree (Table 2). Four simple attributes were combined into eight composite attributes (Table 3), which were divided into tree attributes, crown attributes and shape attributes (Wang et al., 2021).

Secondly, simple attributes and composite attributes were established as input variables for four types of machine learning, along with the configuration of model parameters.As to compare with the

Table 3. Composite attributes and formulas (In the table, S and V are the crown surface area and volume, respectively)

Type	Formula
Tree attributes	$\frac{L_x}{H}$
	$\frac{L_y}{H}$
	$\frac{H_c}{H}$
Crown attributes	$\frac{L_x}{H_c}$
	$\frac{L_y}{H_c}$
	$\frac{L_x}{L_y}$
Shape attributes	S, V

Table 1. Extraction of tree attributes from the point cloud

Tree attributes	Extraction formula	Remarks
H (the height of the tree)	$Z_{max} - Z_{min}$	Z_{max} and Z_{min} are the highest and lowest points for a street tree
L_x (the length of the crown in the east-west direction)	$X_{max} - X_{min}$	X is the east-west direction
L_y (the length of the crown in the north-south direction)	$Y_{max} - Y_{min}$	Y is the north-south direction
H_c (the crown height)	$Z_{maxc} - Z_{minc}$	Z_{maxc} and Z_{minc} are the highest and lowest points of the crown

Table 2. Approximate crown shape and corresponding surface area and volume formula for each tree species (In the table, a represents the average crown width, and b represents the average crown height.) (Wang et al., 2022; Zhu et al., 2021)

Tree attributes	Crown shape	Surface area formula	Volume formula
Koelreuteria paniculata	Hemispherical	$\frac{3\pi a^2}{4}$	$\frac{\pi(3ab^2 - 2b^3)}{12}$
Aesculus chinensis	Spherical	$\frac{\pi a^2}{4} + \pi ab$	$\frac{\pi(3ab^2 - 2b^3)}{6}$
Catalpa bungei	Oval	$\frac{\pi(a^2 + 2ab)}{3}$	$\frac{\pi a^2 b}{6}$
Liriodendron chinense	Spherical	$\frac{\pi a^2}{4} + \pi ab$	$\frac{\pi(3ab^2 - 2b^3)}{6}$
Ginkgo biloba	Conic	$\frac{\pi(a^2 + 2ab)}{4}$	$\frac{\pi a^2 b}{12}$
Firmiana platanifolia	Cylindrical	$\frac{\pi a^2}{2} + \pi ab$	$\frac{\pi a^2 b}{4}$

Table 4. Groups setting in machine learning algorithms. Group 1, 2 and 3 stand for the combination of simple attributes. Group 1C, 2C and 3C are the combinations of simple attributes and their corresponding composite attributes (labeled as bold)

Groups	Group members					
Group 1	(H, H_c)	(H, L_x)	(H, L_y)	(H_c, L_x)	(H_c, L_y)	(L_x, L_y)
Group 1C	$(H, H_c, \frac{H_c}{H})$	$(H, L_x, \frac{L_x}{H})$	$(H, L_y, \frac{L_y}{H})$	$(H_c, L_x, \frac{L_x}{H_c})$	$(H_c, L_y, \frac{L_y}{H_c})$	$(L_x, L_y, \frac{L_x}{L_y})$
Group 2	(H, H_c, L_x)		(H, H_c, L_y)	(H, L_x, L_y)		(H_c, L_x, L_y)
Group 2C	$(H, H_c, L_x, \frac{H_c}{H}, \frac{L_x}{H}, \frac{L_x}{H_c})$		$(H, H_c, L_y, \frac{H_c}{H}, \frac{L_y}{H}, \frac{L_y}{H_c})$	$(H, L_x, L_y, \frac{L_x}{H}, \frac{L_y}{H}, \frac{L_x}{L_y})$		$(H_c, L_x, L_y, \frac{L_x}{H_c}, \frac{L_y}{H_c}, \frac{L_x}{L_y})$
Group 3	(H, H_c, L_x, L_y)					
Group 3C	(H, H_c, L_x, L_y, S, V)			$(H, H_c, L_x, L_y, \frac{H_c}{H}, \frac{L_x}{H}, \frac{L_y}{H}, \frac{L_x}{H_c}, \frac{L_y}{H_c}, \frac{L_x}{L_y})$		

effectiveness of classification by simple attributes and simple attributes adding with composite attributes, simple attributes participate in the classification, named Group1, Group2 and Group3; Group1, Group2 and Group3 adding with corresponding composite attributes are named Group1C, Group2C and Group3C respectively (Table 4). Pre-experiments on parameters which may influence the fitting results was conducted to obtain the optimal parameters for model fitting. The BP neural network was established with two hidden layers; the first layer had 20 neurons, and the second layer had 10 neurons, the alpha parameter was 10^{-5}, and the solver is set as "adam". The value of k in KNN was 1, the value of gamma in SVM is 0.1, and the kernel in SVM is set as "rbf". The ratios of the testing dataset and all datasets were set as 0.3. We set the ratio of training set and test set as 3:7, for all the data, 0.3 is randomly selected as the training set each time, and the remaining 0.7 is used as the test set. The experiment was repeated 100 times and the average of the 100 results was obtained as the final result.

Accuracy assessment

The correlation between attributes extracted from UAV-obtained data and observations was expressed as an R^2 value obtained using R 4.2.1 software. The R^2 values close to 1 indicate a high correlation. The effectiveness of identifying street trees based on composite and simple attributes was assessed with non-paramteric test (Kruskal-Wallis Test) using IBM SPSS Statistics 26. The distribution of the simple attributes and composite attributes have significant differences across categories of group ($P<0.05$, Table 5). The results of Kruskal-Wallis Test are represented with letters; attributes with different letters indicate significant differences among tree species, and those with the same letter indicate not (Jin et al., 2019).

Each experiment was repeated ten times to avoid the impact of the randomness of the validation samples on the accuracy of the BP neural network, KNN and SVM which were implemented using Python 3.9 software (Liang et al., 2020). The accuracy of street tree identification was evaluated by accuracy (%), precision (%), recall value (%), F1 score and kappa coefficient; the corresponding formula is

Table 5. Independent-Samples Kruskal-Wallis test summary (The significance level is 0.050 and the test statistic is adjusted for ties)

	Total N	Test statistic	Degree of freedom	Asymptotic sig. (2-sided test)
H	90	58.988	5	1.97×10^{-11}
L_y		60.143		1.14×10^{-11}
L_x		52.839		3.63×10^{-10}
H_c		50.487		1.10×10^{-9}
L_x/H		60.185		1.11×10^{-11}
L_y/H		46.667		6.64×10^{-9}
H_c/H		46.847		6.10×10^{-9}
L_x/H_c		68.202		2.42×10^{-13}
L_y/H_c		48.615		2.66×10^{-9}
L_x/L_y		57.327		4.33×10^{-11}
S		61.539		5.84×10^{-12}
V		60.782		8.38×10^{-12}

$$\text{Accuracy (\%)} = \frac{TP + TN}{N} \times 100\%$$

$$\text{Precision (\%)} = \frac{TP}{TP + FP} \times 100\%$$

$$\text{Recall value (\%)} = \frac{TP}{TP + FP} \times 100\%$$

$$\text{F1 score} = \frac{2 \times TP}{2 \times TP + FP + FN}$$

$$\text{Kappa coefficient} = \frac{p_o - p_e}{1 - p_e}$$

$$p_e = \frac{a1 \times b1 + a2 \times b2 \ldots aC \times bC}{n \times n}$$

where TP represents the number of samples that are judged to be positive and are actually positive samples; TN is the number of samples that are predicted to be negative samples and are actually negative samples; and N represents the total number of samples; FP represents the number of samples that are judged to be positive samples and are actually false samples; FN represents the number of samples that are judged to be false samples and are actually positive samples; po is accuracy; the real number of samples in each category is a1,a2,... aC, and the predicted number of samples for each category is b1,b2... ,bC.

Results

The accuracy of attribute extraction from UAV data

The attributes extracted from UAV data, including H, L_x, L_y, H_c, S and V, displayed significant correlations with observations, with R^2 values greater than 0.75 (Fig. 3). The R^2 between observations and the extracted values of H reached 0.90. The R^2 between observations and the extracted values of crown width in the east-west direction reached 0.87. The R^2 between observations and the extracted values of the crown width in the north-south direction reached 0.78. The lowest R^2 was observed for H_c at only 0.76. R^2 greater than 0.75 suggests that the UAV can achieve a certain accuracy in the extraction of tree attributes (Hao et al., 2021; Jin et al., 2020). The S and V values calculated based on point cloud extraction and the geometric method also showed high R^2 values of 0.86 and 0.85, respectively, indicating the feasibility of obtaining the S and V values of street trees with the geometric method.

Compared to the relative errors for L_x, L_y and H_c, the relative errors of H showed the smallest values among the six street tree species (Table 6). The average relative errors for all four of these attributes were less than 15%. The largest relative error was observed for H_c at 10.95%. The relative errors of H were the smallest at 5.80% while the relative error of crown width was slightly larger than that of H. The relative errors of L_x and L_y were 9.52% and 8.69%, respectively. Among the four attributes, H showed the least fluctuation while L_y was the largest (Table 6 and Figure 4). In the assessment of the differences among tree species, the relative errors of the

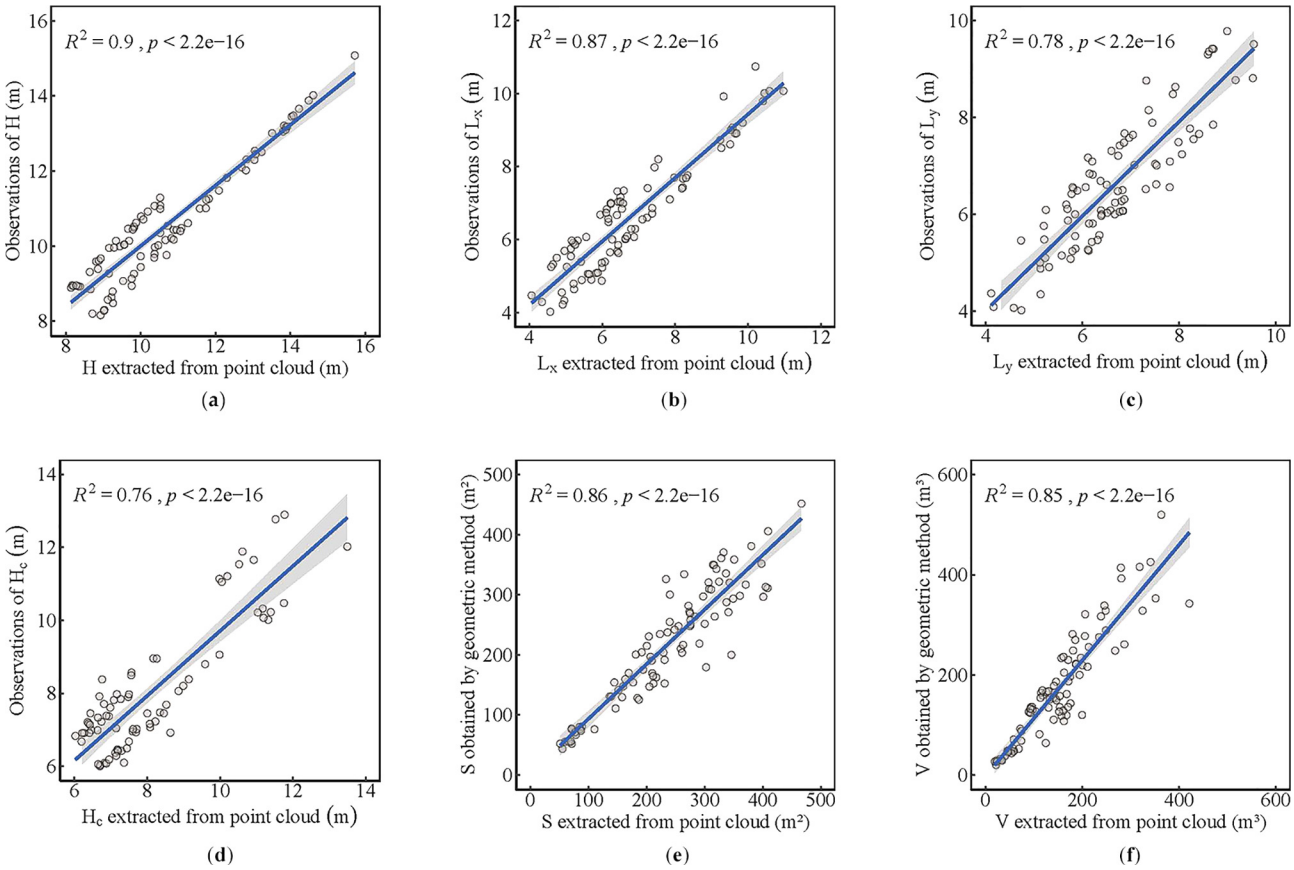

Fig. 3. Accuracy of street tree attribute extraction. (a), (b), (c), and (d) are the correlation analysis results based on point cloud-extracted values and observations, and (e) and (f) are the correlation analysis results based on the point cloud-extracted values and the values obtained with the geometric algorithm. The gray part represents the 95% confidence interval, and the blue line represents the linear relationship between the two sets of values

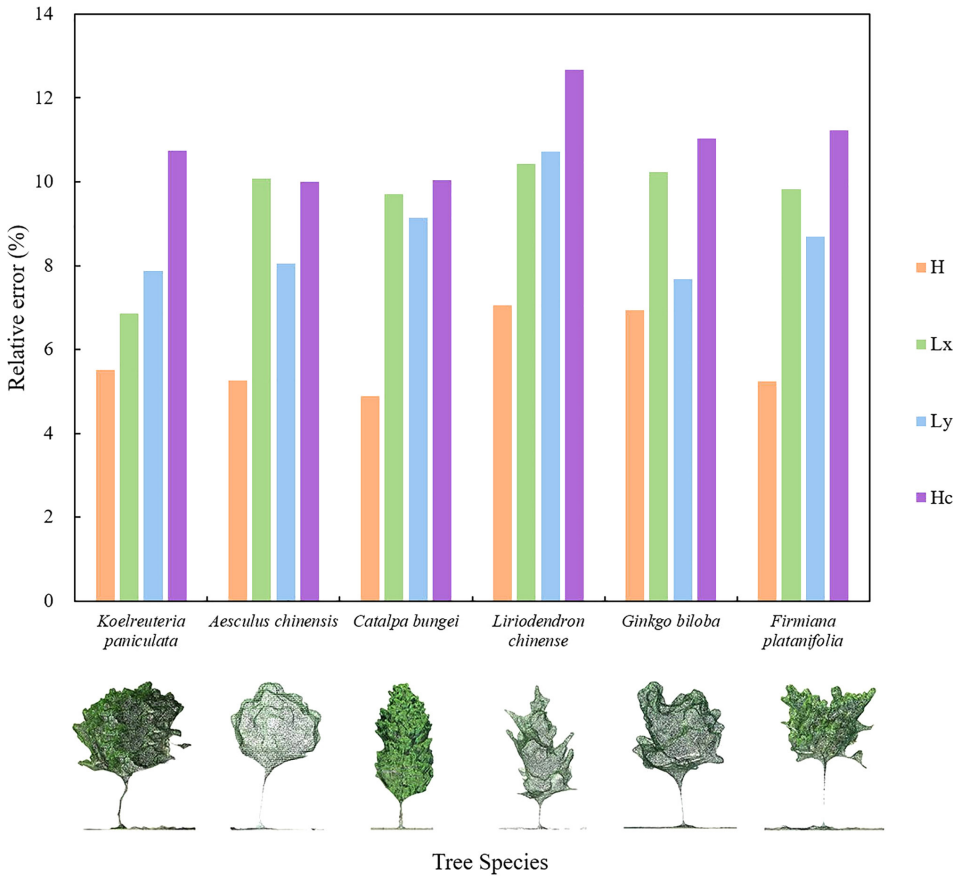

Fig. 4. Relative errors of the four attributes for six tree species (H is tree height, L_x is the length of the crown in the east-west direction, L_y is the length of the crown in the north-south direction, and H_c is crown height)

attributes of the six tree species were less than 14%. The relative errors of the four attributes of *Liriodendron chinense* were greater than those for other tree species, indicating that the extraction accuracy was lowest for *Liriodendron chinense* among the six tree species. The extraction errors for *Firmiana platanifolia* and *Ginkgo biloba* were less than 12% but greater than 11%. Additionally, the relative errors for *Koelreuteria paniculata*, *Aesculus chinensis* and *Catalpa bungei* were less than 11%.

Table 6. Relative errors of the extracted tree attributes (In the table, H is tree height, L_x is the length of the crown in the east-west direction, L_y is the length of the crown in the north-south direction, and H_c is crown height)

Tree attribute	Relative error (%)			RMSE (m)
	Minimum value	Maximum value	Average value	
H	0.76	10.62	5.80±1.89	3.57×10^{-4}
L_x	0.41	22.87	9.52±3.73	1.39×10^{-3}
L_y	0.33	18.93	8.69±4.10	1.68×10^{-3}
H_c	1.46	24.74	10.95±3.59	1.29×10^{-3}

Effectiveness of Characterization based on Composite and Simple Attributes

Compared to the simple attributes, the composite attributes showed more interspecific differences among street tree species. With regard to tree species such as *Aesculus chinensis* and *Liriodendron chinense*, four simple attributes, namely, H, L_x, L_y and H_c, exhibited no significant differences, while composite attributes such as L_x/L_y displayed significant differences between *Aesculus chinensis* and *Liriodendron chinense* (Fig. 5, 6). For simple attributes, the values of H and H_c for *Aesculus chinensis* and *Ginkgo biloba* were similar (Fig.s 5a and 5d). However, the proportions of H and H_c showed remarkable differences among the two tree species, which were easily distinguished (Fig.s 6c). Overall, composite attributes provided information to identify street tree species that simple attributes could not provide.

For simple attributes, *Catalpa bungei* displayed a higher H than *Aesculus chinensis* and *Ginkgo biloba*, with a minimum value of 12.7 m and a maximum value of 15.7 m, and as similar values as *Koelreuteria paniculata*, *Liriodendron chinense* and *Firmiana Platanifolia* (Fig. 5a). The minimum value of L_x for *Koelreuteria paniculata* was 9.3 m, which was higher than

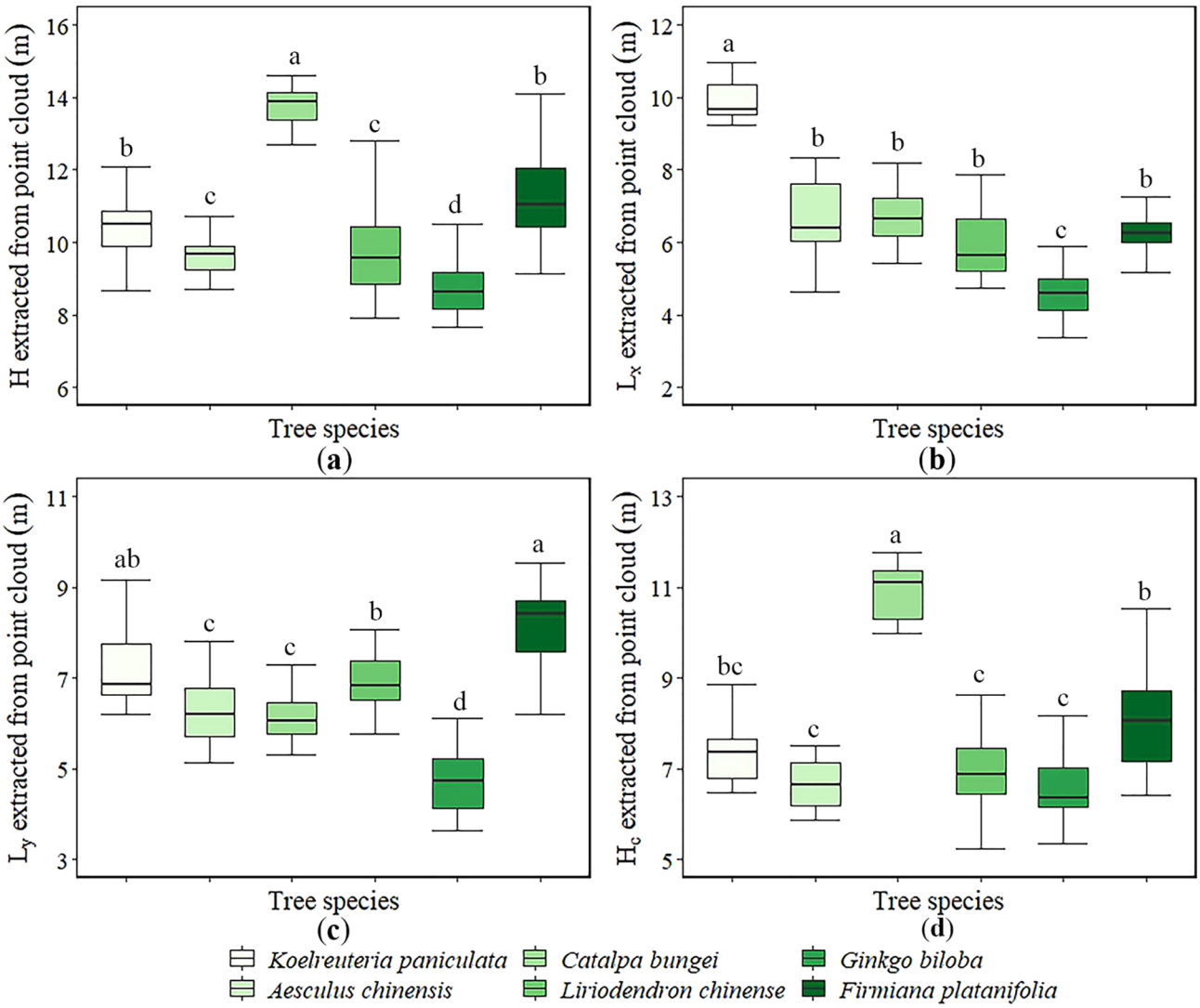

Fig. 5. Kruskal-Wallis test results for the differences in simple attributes among different trees. (a), (b), (c) and (d) are the test results for H (tree height), L_x (the length of the crown in the east-west direction), L_y (the length of the crown in the north-south direction) and H_c (crown height), respectively. Different superscript letters (a, b, c, and d) indicate a significant difference among the means in each row, with $p < 0.05$ for Kruskal-Wallis test

the maximum values for the other five tree species, but the overlap was observed for the other species (Fig. 5b). Additionally, L_y values overlapped for all six tree species, ranging from 3.6 m to 9.6 m (Fig. 5c). *Catalpa bungei* exhibited a higher H_c than *Koelreuteria paniculata*, *Aesculus chinensis*, *Liriodendron chinense* and *Ginkgo biloba*, with a minimum value of 10.0 m and a maximum value of 13.5 m, but the overlap was observed with the corresponding values for *Firmiana Platanifolia* (Fig. 5d).

For composite attributes, *Koelreuteria paniculata* showed higher values of L_x and H than *Catalpa bungei*, *Liriodendron chinense*, *Ginkgo biloba* and *Firmiana Platanifolia*, with a minimum value of 0.82 and a maximum value of 1.19, but overlap was observed with the values for *Aesculus chinensis* (Fig. 6a). Only the L_y/H values of *Aesculus chinensis* and *Catalpa bungei* were different, ranging from 0.55 to 0.77 and 0.40 to 0.54, respectively (Fig. 6b). Additionally, the H_c and H values of *Koelreuteria paniculata* and *Catalpa bungee* were different, ranging from 0.61 to 0.73 and 0.74 to 0.86, respectively, but overlap in these values was observed for the other four tree species (Fig. 6c). *Koelreuteria paniculata* exhibited higher L_x/H_c values than *Catalpa bungei*, *Liriodendron chinense*, *Ginkgo biloba* and *Firmiana Platanifolia*, with a minimum value of 1.11 and a maximum value of 1.82, but overlap was observed with the corresponding values for *Aesculus chinensis* (Fig. 6d). The Ly/Hc range for Koelreuteria paniculate, Aesculus chinensis, and Liriodendron chinense was 0.72 to 1.20, which was higher than the range for Catalpa bungei (0.49 to 0.65) (Fig. 6e). With a minimum value of 1.12 and a maximum value of 1.63, *Koelreuteria paniculata* displayed higher L_x/L_y values than *Liriodendron chinense* and *Firmiana Platanifolia*, with corresponding values ranging from 0.69

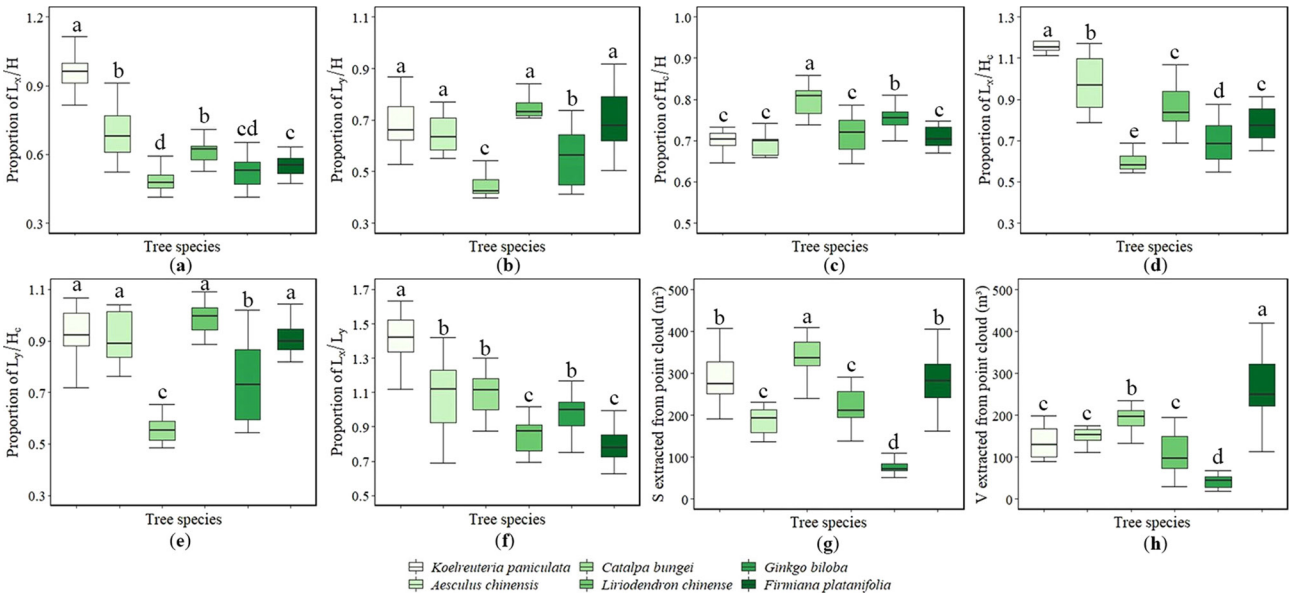

Fig. 6. Kruskal-Wallis test results for the difference in composite attributes among different trees. (a), (b), (c), (d), (e), (f), (g) and (h) are the test results for L_x/H, L_y/H, H_c/H, L_x/H_c, L_y/H_c, L_x/L_y, S and V, respectively. Different superscript letters (a, b, c, d and e) indicate a significant difference among the means in each row, with $p < 0.05$ for Kruskal-Wallis test

to 1.02 and 0.63 to 0.99, respectively (Fig. 6f). The smallest S was associated with *Ginkgo biloba*, with a range from 51.1 to 110.2 m²; these values differed from those for *Koelreuteria paniculata*, *Aesculus chinensis*, *Catalpa bungee*, *Liriodendron chinense* and *Firmiana Platanifolia* by 191.5 to 408.3 m², 136.5 to 346.0 m², 239.9 to 766.7 m², 138.8 to 290.9 m², and 163.2 to 405.0 m² respectively (Fig. 6g). The maximum value of V for *Ginkgo biloba* was 68.8 m³, which was lower than the minimum values for *Koelreuteria paniculata*, *Catalpa bungee* and *Firmiana Platanifolia* but overlapped with the ranges for *Aesculus chinensis* and *Liriodendron chinense* (Fig. 6h).

Accuracy of tree species classification

The accuracy of tree species identification can be improved by adding composite attributes based on simple attributes. We tested two sets of data, one only containing simple attributes and the other with

Table 7. Accuracy comparations in different machine algorithms (Group 1, 2 and 3 stand for the combination of simple attributes. Group 1C, 2C and 3C are the combinations of simple attributes and their corresponding composite attributes)

Machine learning algorithm	Attributes	Accuracy (%)	Precision (%)	Recall value (%)	F1 score	Kappa coefficient
BP neural network	Group 1	33.9	24.4	37.5	0.28	0.22
	Group 1C	50.0	41.6	47.6	0.43	0.39
	Group 2	63.0	58.4	60.6	0.57	0.55
	Group 2C	63.0	58.4	60.6	0.57	0.55
	Group 3	44.4	37.5	47.2	0.33	0.35
	Group 3C	74.1	67.9	70.8	0.69	0.69
K- nearest neighbor	Group 1	33.3	39.9	33.1	0.33	0.20
	Group 1C	53.1	52.9	52.1	0.52	0.43
	Group 2	47.2	47.0	48.6	0.47	0.37
	Group 2C	63.0	66.0	62.2	0.62	0.55
	Group 3	55.6	55.6	54.2	0.55	0.46
	Group 3C	72.3	76.9	70.6	0.72	0.67
Support vector machines	Group 1	33.9	23.5	39.4	0.26	0.23
	Group 1C	57.4	53.8	59.4	0.53	0.50
	Group 2	59.3	49.4	62.5	0.52	0.52
	Group 2C	70.4	74.5	69.3	0.69	0.64
	Group 3	70.4	61.3	72.2	0.63	0.65
	Group 3C	76.0	77.3	74.1	0.74	0.71

simple attributes and composite attributes that related to the simple attributes (Table 7). When four simple attributes were used for classification, SVM showed the highest classification accuracy (70.4%) and kappa coefficient (0.65), followed by KNN and BP neural networks with accuracy is 55.6% and 44.4% and kappa coefficient is 0.46 and 0.35 (Table 7). Compared to the one only containing simple attributes, when simple attributes are combined with their composite attributes, SVM showed the highest classification accuracy (76.0%) with an increase of 5.6%, followed by BP neural network (74.1%) and KNN (72.3%) with an increase of 29.7% and 16.7%, respectively. The kappa coefficients in descending order were SVM (0.71), BP (0.69), and KNN (0.67), with corresponding improvements of 0.06, 0.34, and 0.21. (Table 7). Among the three machine learning algorithms, the most improved is BP neural network. When composite attributes corresponding to simple attributes are included, the classification accuracy of BP neural network is improved by 29.7%, and kappa coefficient is improved by 0.34.

Discussion

In this study, high correlations were obtained between the extracted and observed values with R^2 greater than 0.75, suggesting that the street tree attributes obtained by UAVs are reasonable (Dong et al., 2020; Nasiri et al., 2021). Therefore, UAV-based methods can be a good alternative to traditional measurement methods due to their high accuracy and capacity to obtain large-scale measurements (Charron et al., 2020; Schiefer et al., 2020). Our results showed that R^2 values of H, L_x, L_y and H_c were 0.90, 0.87, 0.78, and 0.76, respectively, which were consistent with a previous study with the reported R^2 values being 0.849 and 0.895 of tree height extracted from a canopy height model at spatial resolutions of 0.2 m and 0.1 m, respectively (Tian et al., 2019). However, one study showed that R^2 value for crown width was 0.66, which is lower than that obtained in this study, likely due to the influence of high tree density on crown shield measurements (Díaz-Varela et al., 2015). In areas where nonground coverage < 0.95, the extraction accuracy of the crown height based on UAV data was high ($R^2 = 0.86–0.94$) (Zhou et al., 2022). Notably, because of the presence of bushes under street trees, the R^2 in this study was lower than those in other studies (Ghanbari Parmehr & Amanti, 2021; Wang et al., 2016; Kaartinen et al., 2012). The high correlation between the extracted values of the crown surface and volume and the results of the geometric method verified the feasibility of using a geometric calculation approach (Anifantis et al., 2019).

The addition of composite attributes improves the accuracy of identification by machine learning algorithm compare with only using simple attributes. Apparently, when using simple attributes, the addition of related composite attributes provides more information and highly improves the classification accuracy of KNN and SVM. The addition of composite attributes improves the results of the three machine learning algorithms to different degrees. Among the three machine algorithms, BP neural network has the highest accuracy improvement with the addition of combined attributes. When H, H_c, L_x and L_y are used, the classification accuracy of BP neural network was only 44.4% (kappa coefficient is 0.35), and the classification accuracy was increased by 29.7% (kappa coefficient is increased by 0.34) after adding the composite attributes related to these four attributes. This suggested that the addition of composite attributes reduces interspecific confusion. SVM showed the highest classification accuracy whether using simple attributes or simple attributes with additional composite attributes. The BP neural network is logically based and is minimally affected by the sample size (Fassnacht et al., 2016). When composite attributes are included, the length provided by simple attributes and the shape provided by composite attributes enhance the logicality of BP neural network and improve its classification accuracy.

A combination of multiple remote-sensing data can greatly improve the classification of street species (Liao et al., 2018; Lee et al., 2021). For example, multispectral/hyperspectral data contain rich texture and phenological features (Fassnacht et al., 2016). The LiDAR can penetrate trees so that more understory data can be obtained (Zou et al., 2020). UAV tilt photography is convenient to obtain more geometric information (Ren et al., 2019). The utilization of Airborne LiDAR technology has garnered increasing attention for 3D assessments of forest structures, ranging from individual tree-level analyses to landscape-scale evaluations. Data fusion of texture information and geometric information extracted by LiDAR or UAV may benefit tree species classification, which is strongly recommended in the future study (Alonzo et al., 2014). Furthermore, in the realm of deep learning, the opportunity to refine accuracy through network training arises when an ample quantity of sample data is present to construct a comprehensive sample database (Lumnitz et al., 2021; Martins et al., 2021). However, there is no relative published trainsets that can be used in the deep learning. While in our study or similar experiments, multiple simple attributes such as L_x, L_y and H_c has to be manually extracted, which is time-consuming step and difficult to meet the number requirements for deep learning. In the future, we will explore the

way to fast extract simple attributes at a large scale so that a sample database can be built for large-scale urban street tree classification.

Conclusions

In this study, we explored the street tree attributes obtained by UAVs and assessed the effectiveness of tree species characterization and identification based on composite attributes (two or more simple attributes) and simple attributes. The result indicated that the attributes obtained by UAVs are effective, and composite attributes displayed more interspecific differences among street trees than simple attributes did. The use of composite attributes resulted in higher interspecific differences among street trees than simple attributes did, indicating that composite attributes enhance the characterization of street tree attributes. Four tree species showed insignificant differences in Lx and Hc, and three species showed insignificant differences in H, Ly and V (Fig. 5). Tree species exhibited high similarity based on simple attributes, which caused confusion in identification. However, both small and large differences were observed when composite attributes were considered, thus enhancing the identification of differences among trees. Lx/Ly could be used to clearly identify Aesculus chinensis and Liriodendron chinense, which could not be identified with the four simple attributes. Thus, the two trees had similar Lx and Ly values, but the proportions of Lx and Ly varied. Composite attributes provided information that simple attributes could not, and this information was useful for identifying street tree species. The accuracy of simple attributes when combined withcomposite attributes for tree species classification is about 3.70% to 26.0% higher than that of simple attributes alone. As a potential combination attribute, S and V can improve the classification accuracy of simple attributes. Among the three classifiers, SVM has the highest classification accuracy, the BP neural network has the largest accuracy improvement after the influence of composite attributes. The method applied in this study provides an effective alternative for using composite attributes and UAV technology to obtain street tree species information and increase the accuracy of street tree identification for large-scale street tree monitoring and detailed management.

Author Contributions

Conceptualization, Hongke Hao and Hongying Tang; investigation, Fan Miao, Bingyu Wu and Jie Yang; methodology, Hongke Hao and Hongying Tang; resources, Hongke Hao; software, Hongying Tang, Fan Miao, Jie Yang, Bingyu Wu and Qi Zhang; validation, Hongke Hao; formal analysis, Hongying Tang and Hongke Hao; data curation, Hongke Hao and Hongying Tang; writing–original draft preparation, Hongke Hao, Hongying Tang, Fan Miao, Jie Yang, Bingyu Wu and Qi Zhang; visualization, Jie Yang and Qi Zhang. All authors have read and agreed to the published version of the manuscript.

Funding

This research received no external funding.

Institutional review board statement

Not applicable.

Informed consent statement

Not applicable.

Data availability statement

The data presented in this study are available in https://drive.google.com/file/d/1d6_pbb5R7cGwWE1MDjsJ5R9lhwJ6V7vm/view?usp=sharing.

Conflicts of interest

The authors declare no conflict of interest.

References

Abbas S, Peng Q, Sing Wong M, Li Z, Wang J, Tze Kwun Ng K, Yin Tung Kwok C & Ka Wai Hui K (2021) Characterizing and classifying urban tree species using bi-monthly terrestrial hyperspectral images in Hong Kong. ISPRS Journal of Photogrammetry and Remote Sensing 177: 204–216. doi:10.1016/j.isprsjprs.2021.05.003.

Alonzo M, Bookhagen B & Roberts DA (2014) Urban tree species mapping using hyperspectral and lidar data fusion. Remote Sensing of Environment 148: 70–83. doi:10.1016/j.rse.2014.03.018.

Aminipouri M, Knudby AJ, Krayenhoff ES, Zickfeld K & Middel A (2019a) Modelling the impact of increased street tree cover on mean radiant temperature across Vancouver's local climate zones. Urban Forestry & Urban Greening 39: 9–17. doi:10.1016/j.ufug.2019.01.016.

Aminipouri M, Rayner D, Lindberg F, Thorsson S, Knudby AJ, Zickfeld K, Middel A & Krayenhoff ES (2019b) Urban tree planting to maintain outdoor thermal comfort under climate change: The case of Vancouver's local climate zones. Building and

Environment 158: 226–236. doi:10.1016/j.buildenv.2019.05.022.

Anifantis AS, Camposeo S, Vivaldi GA, Santoro F & Pascuzzi S (2019) Comparison of UAV photogrammetry and 3D modeling techniques with other currently used methods for estimation of the tree row volume of a super-high-density olive orchard. Agriculture 9: 233. doi:10.3390/agriculture9110233.

Aval J, Demuynck J, Zenou E, Fabre S, Sheeren D, Fauvel M, Adeline K & Briottet X (2018) Detection of individual trees in urban alignment from airborne data and contextual information: A marked point process approach. ISPRS Journal of Photogrammetry Remote Sensing 146: 197–210. doi:10.1016/j.isprsjprs.2018.09.016.

Charron G, Robichaud-Courteau T, La Vigne H, Weintraub S, Hill A, Justice D, Bélanger N & Lussier Desbiens A (2020) The DeLeaves: a UAV device for efficient tree canopy sampling. Journal of Unmanned Vehicle Systems 8: 245–264. doi:10.1139/juvs-2020-0005.

Chen YL, Wu CC & Tang K (2009) Building a cost-constrained decision tree with multiple condition attributes. Information Sciences 179: 967–979. doi:10.1016/j.ins.2008.11.032.

Choudhury MAM, Marcheggiani E, Despini F, Costanzini S, Rossi P, Galli A & Teggi S (2020) Urban tree species identification and carbon stock mapping for urban green planning and management. Forests 11: 1226. doi:10.3390/f11111226.

Cowett F & Bassuk NL (2020) Street tree diversity in Massachusetts, USA. Arboriculture Urban Forestry & Urban Greening 46: 27–43. doi:10.48044/jauf.2020.003.

Dai C (2015) The predicting models of crown volume and crown surface area about main species of tree of Beijing. North China University of Science and Technology, Qinhuangdao, China.

Díaz-Varela R, Rosa RDl, León L & Zarco-Tejada P (2015) High-resolution airborne UAV imagery to assess olive tree crown parameters using 3D photo reconstruction: application in breeding trials. Remote Sensing 7: 4213–4232. doi:10.3390/rs70404213.

Dong X, Zhang Z, Yu R, Tian Q & Zhu X (2020) Extraction of information about individual trees from high-spatial-resolution UAV-acquired images of an orchard. Remote Sensing 12: 133. doi:10.3390/rs12010133.

Duizer LM, Bloom K & Findlay CJ (1997) Dual-attribute time-intensity sensory evaluation: A new method for temporal measurement of sensory perceptions. Food Quality and Preference 8: 261–269. doi:10.1016/S0950-3293(96)00052-3.

Fassnacht FE, Latifi H, Stereńczak K, Modzelewska A, Lefsky M, Waser LT, Straub C & Ghosh A (2016) Review of studies on tree species classification from remotely sensed data. Remote Sensing of Environment 186: 64–87. doi:10.1016/j.rse.2016.08.013.

Franklin SE & Ahmed OS (2018) Deciduous tree species classification using object-based analysis and machine learning with unmanned aerial vehicle multispectral data. International Journal of Remote Sensing 39: 5236–5245. doi:10.1080/01431161.2017.1363442.

Ghanbari Parmehr E & Amanti M (2021) Individual tree canopy parameters estimation using UAV-based photogrammetric and LiDAR point clouds in an urban park. Remote Sensing 13: 2062. doi:10.3390/rs13112062.

Da-tong X (2015) Methodology on history of forestry science and technology in China. Journal of Beijing Forestry University (Social Sciences) 14: 14–16.

Guo YS, Zhang HS, Li QS, Lin YY & Joseph M (2022) New morphological features for urban tree species identification using LiDAR point clouds. Urban Forestry & Urban Greening 71: 127558. doi:10.1016/J.UFUG.2022.127558.

Hao Z, Lin L, Post CJ, Jiang Y, Li M, Wei N, Yu K & Liu J (2021) Assessing tree height and density of a young forest using a consumer unmanned aerial vehicle (UAV). New Forests 52: 843–862. doi:10.1007/s11056-020-09827-w.

Jin C, Oh C-y, Shin S, Wilfred Njungwi N & Choi C (2020) A comparative study to evaluate accuracy on canopy height and density using UAV, ALS, and fieldwork. Forests 11: 241. doi:10.3390/f11020241.

Jin S, Kim D-Y, Kim J-H & Kim W-C (2019) Accuracy of dental replica models using photopolymer materials in additive manufacturing: In vitro three-dimensional evaluation. Journal of Prosthodontics 28: 557–562. doi:10.1111/jopr.12928.

Jombo S, Adam E & Odindi J (2021) Classification of tree species in a heterogeneous urban environment using object-based ensemble analysis and World View-2 satellite imagery. Applied Geomatics 13: 373–387. doi:10.1007/S12518-021-00358-3.

Kaartinen H, Hyyppä J, Yu X, Vastaranta M, Hyyppä H, Kukko A, Holopainen M, Heipke C, Hirschmugl M, Morsdorf F, Næsset E, Pitkänen J, Popescu S, Solberg S, Wolf BM & Wu JC (2012) An international comparison of individual tree detection and extraction using airborne laser scanning. Remote Sensing 4: 950–974. doi:10.3390/rs4040950.

Kraidech S & Jearanaitanakij K (2017) Improving ID3 algorithm by combining values from equally important attributes: 2017 21st International Computer Science and Engineering

Conference (ICSEC), pp. 1–5. doi:10.1109/ICSEC.2017.8443862.

Lai Y & Kontokosta CE (2019) The impact of urban street tree species on air quality and respiratory illness: A spatial analysis of large-scale, high-resolution urban data. Health and Place 56: 80–87. doi:10.1016/j.healthplace.2019.01.016.

Li Y (2022) Health and safety evaluation of street trees in Xi 'an, Vol. master: Northwest A-F University, Yangling.

Liang Z, Li Z, Lai K, Lin Z, Li T & Zhang J (2020) Application of 10-fold cross-validation in the evaluation of generalization ability of prediction models and the realization in R. Chinese Journal of Hospital Statistics 27: 289–292.

Liao W, Van Coillie F, Gao L, Li L, Zhang B & Chanussot J (2018) Deep learning for fusion of APEX hyperspectral and full-waveform LiDAR remote sensing data for tree species mapping. IEEE Access 6: 68716–68729. doi:10.1109/ACCESS.2018.2880083.

Lee LSH, Zhang H & Jim CY (2021) Serviceable tree volume: An alternative tool to assess ecosystem services provided by ornamental trees in urban forests. Urban Forestry & Urban Greening 59: 127003. doi:10.1016/j.ufug.2021.127003.

Lumnitz S, Devisscher T, Mayaud JR, Radic V, Coops NC & Griess VC (2021) Mapping trees along urban street networks with deep learning and street-level imagery. Isprs Journal of Photogrammetry and Remote Sensing 175: 144–157. doi:10.1016/j.isprsjprs.2021.01.016.

Martins GB, Cue La Rosa LE, Happ PN, Teixeira Coelho Filho LC, Santos CJF, Feitosa RQ & Ferreira MP (2021) Deep learning-based tree species mapping in a highly diverse tropical urban setting. Urban Forestry & Urban Greening 64: 127241. doi:10.1016/j.ufug.2021.127241.

Michałowska M & Rapiński J (2021) A review of tree species classification based on airborne LiDAR data and applied classifiers. Remote Sensing 13: 353. doi:10.3390/RS13030353.

Nasiri V, Darvishsefat AA, Arefi H, Pierrot-Deseilligny M, Namiranian M & Le Bris A (2021) Unmanned aerial vehicles (UAV)-based canopy height modeling under leaf-on and leaf-off conditions for determining tree height and crown diameter (case study: Hyrcanian mixed forest). Canadian Journal of Forest Research 51: 962–971. doi:10.1139/cjfr-2020-0125.

Navarro A, Young M, Allan B, Carnell P & Ierodiaconou D (2020) The application of Unmanned Aerial Vehicles (UAVs) to estimate above-ground biomass of mangrove ecosystems. Remote Sensing of Environment 242: 111747. doi:10.1016/j.rse.2020.111747.

Nevalainen O, Honkavaara E, Tuominen S, Viljanen N, Hakala T, Yu X, Hyyppä J, Saari H, Pölönen I, Imai NN & Tommaselli AMG (2017) Individual tree detection and classification with UAV-Based photogrammetric point clouds and hyperspectral imaging. Remote Sensing 9: 185. doi:10.3390/rs9030185.

Ow LF, Ghosh S & Mohd YML (2018) Effects of varying establishment approaches on the growth of urban street trees. Arboricultural Journal 40: 201–209. doi:10.1080/03071375.2018.1528092.

Pu R & Landry S (2012) A comparative analysis of high spatial resolution IKONOS and WorldView-2 imagery for mapping urban tree species. Remote Sensing of Environment 124: 516–533. doi:10.1016/j.rse.2012.06.011.

Qin L, Mao P, Xu Z, He Y, Yan C, Hayat M & Qiu G (2022) Accurate Measurement and Assessment of Typhoon-Related Damage to Roadside Trees and Urban Forests Using the Unmanned Aerial Vehicle. Remote Sensing 14: 2093. doi:10.3390/RS14092093.

Raczko E & Zagajewski B (2017) Comparison of support vector machine, random forest and neural network classifiers for tree species classification on airborne hyperspectral APEX images. European Journal of Remote Sensing 50: 144–154. doi:10.1080/22797254.2017.1299557.

Ren J, Chen X & Zheng Z (2019) Future Prospects of UAV Tilt Photogrammetry Technology. IOP Conference Series: Materials Science and Engineering 612: 032023. doi:10.1088/1757-899X/612/3/032023.

Schiefer F, Kattenborn T, Frick A, Frey J, Schall P, Koch B & Schmidtlein S (2020) Mapping forest tree species in high resolution UAV-based RGB-imagery by means of convolutional neural networks. Isprs Journal of Photogrammetry and Remote Sensing 170: 205–215. doi:10.1016/j.isprsjprs.2020.10.015.

Su D & Gao X (2020) Estimation of forest canopy density and stock volume based on UAV aerial survey Data. Journal of Forestry Engineering 5: 156–163. doi:10.13360/j.issn.2096-1359.201904031.

Tan 0058 & Shibata S (2022) Factors influencing street tree health in constrained planting spaces: Evidence from Kyoto City, Japan. Urban Forestry & Urban Greening 67: 127416. doi:10.1016/J.UFUG.2021.127416.

Tian J, Dai T, Li H, Liao C, Teng W, Hu Q, Ma W & Xu Y (2019) A novel tree height extraction approach for individual trees by combining TLS and UAV image-based point cloud integration. Forests 10: 537. doi:10.3390/f10070537.

Wang Y, Hyyppä J, Liang X, Kaartinen H, Yu X, Lindberg E, Holmgren J, Qin Y, Mallet C, Ferraz A, Torabzadeh H, Morsdorf F, Zhu L, Liu J & Alho

P (2016) International benchmarking of the individual tree detection Methods for modeling 3-D canopy structure for silviculture and forest ecology using airborne laser scanning. IEEE Trans. Geoscience and Remote Sensing 54: 5011–5027. doi:10.1109/TGRS.2016.2543225.

Wang Y, Wang J, Chang S, Sun L, An L, Chen Y & Xu J (2021) Classification of street tree species using UAV tilt photogrammetry. Remote Sensing 13: 216. doi:10.3390/rs13020216.

Wang YT, Wang J, Niu LW, Chang SP & Sun L (2022) Comparative analysis of extraction algorithms for crown volume and surface area using UAV tilt photogrammetry. Journal of Forestry Engineering 7: 166–173. doi:10.13360/j.issn.2096-1359.202108033.

Zhang BT (2020) Quantitative analysis of ecological benefits on common street trees in the Guanzhong Area. Vol. Master: Northwest A&F University, Yangling.

Zhang C, Xia K, Feng H, Yang Y & Du X (2021) Tree species classification using deep learning and RGB optical images obtained by an unmanned aerial vehicle. Journal of Forestry Research 32: 1879–1888. doi:10.1007/s11676-020-01245-0.

Zhang H, Berg AC, Maire M & Malik J (2006) SVM-KNN: Discriminative nearest neighbor classification for visual category recognition. Vol. 2: Proceedings of the IEEE Computer Society Conference on Computer Vision and Pattern Recognition. doi:10.1109/CVPR.2006.301.

Zhou L, Meng R, Tan Y, Lv Z, Zhao Y, Xu B & Zhao F (2022) Comparison of UAV-based LiDAR and digital aerial photogrammetry for measuring crown-level canopy height in the urban environment. Urban Forestry & Urban Greening 69: 127489. doi:10.1016/J.UFUG.2022.127489.

Zhu Z, Kleinn C & Nöelke N (2021) Assessing tree crown volume - a review. Forestry 94: 18–35. doi:10.1093/forestry/cpaa037.

Zong H, Yao M, Tang Y & Chen H (2020) Assessing the composition, diversity, and allergenic risk of street trees in Qingyang District of Chengdu City. Urban Forestry & Urban Greening 54: 126747. doi:10.1016/j.ufug.2020.126747.

Zou F, Fu Z, Aidi L & Qiang W (2020) Comparative analysis of new forest resources survey methods. Journal of Physics: Conference Series 1646: 012007. doi:10.1088/1742-6596/1646/1/012007.